Impact of Localized Radiative Loss on Inertial Confinement Fusion Implosions

A. Pak,[1] L. Divol,[1] C. R. Weber,[1] L. F. Berzak Hopkins,[1] D. S. Clark,[1] E. L. Dewald,[1] D. N. Fittinghoff,[1] V. Geppert-Kleinrath,[2] M. Hohenberger,[1] S. Le Pape,[1] T. Ma,[1] A. G. MacPhee,[1] D. A. Mariscal,[1] E. Marley,[1] A. S. Moore,[1] L. A. Pickworth,[1] P. L. Volegov,[2] C. Wilde,[2] O. A. Hurricane,[1] and P. K. Patel[1]
[1]*Lawrence Livermore National Laboratory, Livermore, California 94550, USA*
[2]*Los Alamos National Laboratory, Los Alamos, New Mexico 87545, USA*

(Received 21 June 2019; revised manuscript received 18 February 2020; accepted 18 March 2020; published 6 April 2020)

The impact to fusion energy production due to the radiative loss from a localized mix in inertial confinement implosions using high density carbon capsule targets has been quantified. The radiative loss from the localized mix and local cooling of the reacting plasma conditions was quantified using neutron and x-ray images to reconstruct the hot spot conditions during thermonuclear burn. Such localized features arise from ablator material that is injected into the hot spot from the Rayleigh-Taylor growth of capsule surface perturbations, particularly the tube used to fill the capsule with deuterium and tritium fuel. Observations, consistent with analytic estimates, show the degradation to fusion energy production to be linearly proportional to the fraction of the total emission that is associated with injected ablator material and that this radiative loss has been the primary source of variations, of up to 1.6 times, in observed fusion energy production. Reducing the fill tube diameter has increased the ignition metric $\chi_{\mathrm{no}\,\alpha}$ from 0.49 to 0.72, 92% of that required to achieve a burning hot spot.

DOI: 10.1103/PhysRevLett.124.145001

Creating a controlled fusion reaction that produces more energy than supplied to initiate it is a grand scientific challenge [1]. While several approaches to achieve this are being pursued [2,3], each method seeks to couple energy from an external source into a plasma in order to start a cascade of fusion reactions. Recently, the indirect drive inertial confinement fusion (ICF) approach [4] has improved the fusion energy output from implosion experiments by >100 times, with fusion energies up to ~55 kJ having been produced [5,6]. This was achieved by identifying and reducing degradation mechanisms that limit the energy coupling into the reacting plasma [7,8]. While the fusion energy produced was twice the peak kinetic energy of the imploding shell, it is only a few percent of the initial energy supplied to the system. To increase the fusion energy output, understanding and mitigating the impact of the remaining degradation mechanisms is of paramount importance.

Enhanced radiative loss from impurities that mix into the reacting deuterium tritium (DT) plasma is one of the principle degradation mechanisms that reduces fusion energy production [9,10]. In more recent and higher performing implosions conducted with high density carbon (HDC) capsule targets [11,12], improvements to the hydrodynamic stability have decreased the excess emission from contaminants below the detectable level of ~50% [13]. However, spatially resolved x-ray images show bright localized features within the DT plasma with enhanced levels of radiative loss. The spatially localized nature of this emission allows it to be quantified with respect to the hot spot, and it is found to make up ~10%–20% of the total volume but accounts for up to ~50% of the total emission. In contrast to previous work, these features arise from the density perturbation induced by the tube used to fill the capsule with DT fuel and from localized capsule imperfections [14–16].

In this Letter, we quantify for the first time the impact of radiative loss from localized features to fusion energy production in ICF implosion experiments. Understanding the impact of one of the multiple degradation mechanisms that exist is a critical outstanding problem, as the decrease to fusion energy production from each degradation are coupled to one another and to the amount of alpha particle heating. Untangling this interdependence is required to assess the relative importance of each degradation and how it affects the proximity to ignition. Using x-ray and neutron images from multiple lines of sight, 3D reconstructions of the plasma density and temperature for both DT and mix species are created. This allows for the radiative loss from the injected ablator material to be inferred and the impact of the localized cooling of the plasma within the mixed region to be visualized. We find that reducing the diameter of the fill tube by a factor of 2 times resulted in a reduction of the observed fraction of the mix to the total radiative loss by 1.7 times and an increase of 1.6 times in the inferred alpha particle deposited energy and observed fusion energy output. The impact to the proximity to ignition can be estimated using the ignition metric $\chi_{\mathrm{no}\,\alpha}$ which relates the achieved implosion conditions to the Lawson criterion [17]. A burning hot spot is achieved when the energy deposited

from alpha heating exceeds the compressional work done to the reacting plasma and occurs for yield amplifications $\gtrsim 3.5$ and $\chi_{\mathrm{no}\,\alpha} \sim 0.78$. A so-called burning plasma is achieved when alpha particle energy deposition exceeds the compressional work done to the hot spot and confining shell at yield amplifications of ~ 10 and $\chi_{\mathrm{no}\,\alpha} \sim 0.9$. Reducing the fill tube perturbation has increased the ignition metric $\chi_{\mathrm{no}\,\alpha}$ from 0.49 to 0.72, which is 92% of that required to enter into the burning hot spot regime and reduced the proximity to a burning plasma by ~50%. An analytic model is developed that incorporates the degradation to implosion performance using the observed fraction of the total emission associated with the mix. This model indicates that radiative loss has been one of the dominant degradation mechanisms. Informed by this work, improved modeling of the fill tube degradation indicates that reducing the fill tube diameter to 2 μm is essential, but is not sufficient for achieving ignition with the current designs.

In experiments discussed here, the National Ignition Facility (NIF) [18] laser was used to irradiate the inner surface of a uranium hohlraum with up to 1.7 MJ of energy and peak powers up to 450 TW [6]. This produces a near black body x-ray flux with a peak temperature of ~290 eV that compresses a centrally located spherical capsule target. A diagram and radiograph of the HDC capsule used is shown in Fig. 1(b). X-ray ablation of the capsule results in an inward radial compression of the remaining ablator and DT fuel of the target by ~30 times. This creates a central hot spot, wherein DT ions fuse due to the compression and heating resulting from the work done by the imploding shell.

The impact of the fill tube perturbation was studied in a pair of experiments conducted with the same drive and capsule conditions, deliberately changing only the fill tube diameter from 10 to 5 μm, on experiment N170821 and N170601, respectively. As the fill tube diameter was decreased, the neutron yield increased 1.6 times from 1.01×10^{16} to 1.65×10^{16} and the average DT ion temperature increased from 4.2 ± 0.12 to 4.5 ± 0.13 keV.

Coincident with the increase in neutron yield, broad band emission x-ray images taken at photon energies > 10 keV [Figs. 1(c) and 1(d)] show that the localized enhancement of radiative loss from the fill tube perturbation decreased as the fill tube diameter was reduced from 10 to 5 μm. The emission from the fill tube perturbation was quantified using a 2D Fourier filter [21] to remove the lower frequency background DT emission. In this manner, the fill tube emission was found to be 0.43 ± 0.03 and 0.25 ± 0.02 of the total emission for the 10 and 5 μm experiment, respectively. Analysis of time resolved and time integrated images result in comparable mix emission ratios [22].

Using x-ray and neutron images taken from multiple lines of sight, as seen in Fig. 1(e), the properties of the injected mixed ablator material, the subsequent radiative loss, and the impact to the hot spot conditions were inferred. Using the two orthogonal temporally integrated neutron images, the 3D neutron emissivity was first reconstructed [23]. From this, the 3D temperature and density of the DT plasma were inferred assuming an

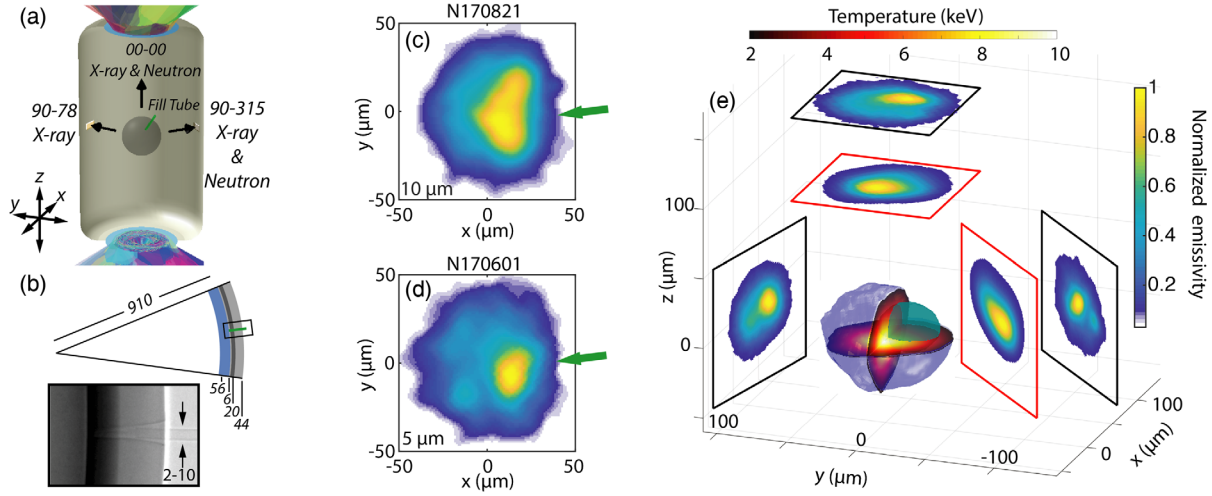

FIG. 1. (a) Experimental setup showing the hohlraum and capsule target. X-ray and neutron images are taken along three and two lines of sight, respectively [19,20]. The polar and azimuthal angle for each detector are denoted. The fill tube enters the capsule at an angle of 90-07 as indicated by the green line. (b) Illustration and radiograph of the initial capsule with dimensions given in μm. The light and dark gray regions denote the undoped, doped with an atomic fraction of 0.33% of tungsten layers of the HDC ablator, respectively. The blue region denotes the DT ice layer. (c),(d) Observed x-ray emission along the 00-00 line of sight at stagnation integrated over ~125 ps for experiments conducted with a 10 and 5 μm fill tube, respectively. The green arrow indicates the initial orientation of the fill tube. (e) 3D reconstruction of the hot spot temperature (>2 keV) for N170601 produced using two temporally integrated neutron emission measurements (outlined in red). Using three x-ray images (outlined in black) the region of localized mix within the hot spot can be reconstructed and is shown by the green contour.

isobaric hot spot, and by matching the observed neutron spectrum and emission width [24]. Figure 1(e) shows the 3D reconstructed DT ion temperature, with the outer blue surface representing the 2 keV isocontour that contains $> 90\%$ of yield. From the reconstructed DT density and temperature quantities, synthetic x-ray images are produced using the DCA [25] emissivity for the DT plasma and taking into account the inferred optical depth of the remaining ablator, image filtration, and the detector response. Compared to the observed x-ray emission images, the synthetic images are found to lack the bright localized x-ray emission produced by the higher atomic number injected ablator material. An ellipsoidal mixed volume, denoted by the green contour in Fig. 1(e), is then added to the reconstructed hot spot. Within this volume, the temperature and pressure of the mix is assumed to be equilibrium with the colocated DT. Measurements of the electron temperature of the mix are being developed to refine the estimate of radiative loss [26,27]. Within the ellipsoid, the number density of mix ions is allowed to vary and adjusted spatially in order to match the emission profiles of the DT + mix emission observed profiles along the three lines of sight seen in Fig. 1(e). From this analysis, the mass and radiative loss of injected mix material and the resulting impact to the DT hot spot conditions can be inferred.

The central plane of the DT hot spot temperature and the region of mix injected by the fill tube perturbation for N170821 and N170601 as produced from 3D reconstructions are shown in Fig. 2. In both experiments, the peak ion temperature is offset from the region of mix, indicating a local cooling of the hot spot [22]. Interestingly, a similar radiative loss from the injected mix is found in both

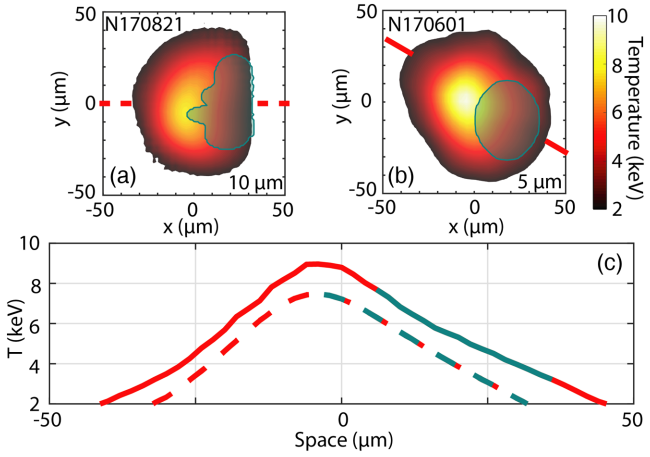

FIG. 2. (a),(b) Profiles of hot spot temperature for experiments N170821 and N170601 conducted with a 10 and 5 μm fill tube, respectively. The shaded region indicates the region of fill tube mix. The dashed and solid lines indicate the direction along which the temperature profile in (c) are taken. The over-plotted dashed and solid green lines denote the location of the mixed material.

experiments despite the 1–1.5 keV difference in temperature [Fig. 2(c)] and the 1.6 times change in yield. The radiative loss is calculated for photon energies >2 keV that are not expected to be reabsorbed within the hot spot and is estimated to be 590 ± 230 and 500 ± 190 joules of energy for N170821 and N170601, respectively. While similar levels of radiative loss were inferred, the amount of injected ablator material on N170821 was larger, being 93 ± 37 ng as compared to 55 ± 22 ng, inferred for N170601.

The larger amount of injected mix mass on the experiment with the 10 μm fill tube increases the rate of radiative loss, reducing the hot spot temperature, amount of alpha heating, and yield as compared to the experiment with the 5 μm fill tube [22]. This effect is described by the power balance of the DT hot spot and can be written [28] as

$$c_{DT}\frac{dT}{dt} = Q_{\alpha} - Q_{\mathrm{rad}} - Q_{\mathrm{cond}} + Q_{\mathrm{PdV}}. \quad (1)$$

Here, c_{DT} is the DT specific heat capacity, T is hot spot temperature, Q_{cond}. is the rate of conductive energy loss, and Q_{PdV} is the rate of mechanical work done on $(Q_{\mathrm{PdV}} > 0)$ or by $(Q_{\mathrm{PdV}} < 0)$ the hot spot. The radiative loss rate can be written as $Q_{\mathrm{rad}} = Q_{\mathrm{DT}} + Q_{\mathrm{mix}}$, and is the sum of the mix and DT emission components. The enhancement to Q_{rad}. from the mix is directly proportional to the amount of mix mass. Equation (1) indicates that different amounts of injected mix mass can produce similar absolute levels of radiative loss, while reducing the temperature and fusion energy production of the reacting DT plasma by different amounts. Therefore, to capture the impact radiative loss has on performance, it is insightful to look at an observed emission mix fraction, defined as the ratio of the emission from the mix to the total emission (DT + mix).

Figure 3(a) shows the fusion yield is observed to decrease monotonically as a function of observed emission mix fraction. These five experiments were conducted with the same capsule and drive conditions. The red data indicates experiments conducted with 5 μm fill tubes. On two of these experiments, lower yields and larger mix fractions were obtained in conjunction with the observation of additional sources of localized mix that arise from capsule perturbations. Figure 3(a) also shows that an additional experiment conducted with a smaller 2 μm diameter fill tube was performed. While a reduction in the observed mix fraction and injected mix mass was seen, the yield did not increase beyond the maximum yield obtained with the larger 5 μm fill tube [22]. A series of 2D simulations was performed using the radiation hydrodynamic code HYDRA [22,29], wherein the fill tube perturbation was increased while holding constant the other degradations. The open black squares in Fig. 3(a) show that the trend in yield degradation with observed emission mix fraction is qualitatively similar in calculations

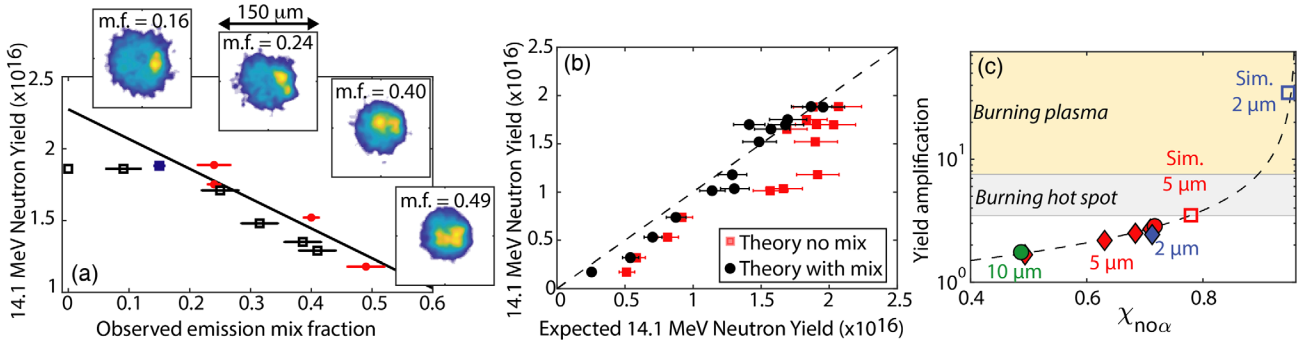

FIG. 3. (a) Yield vs observed emission mix fraction for five experiments with same drive conditions. The fill tube diameter was 2 and 5 μm for the blue and red data, respectively. Open black squares are the observed emission mix fractions of simulated x-ray images from implosions with increasing fill tube diameters (0, 2, 5, 10, 15, 20 μm). The solid line represents the best linear fit to the data. Images of the x-ray emission with energies >10 keV for the different observed mix fractions are also shown. (b) Observed yield vs expected yield using Eq. (2), with and without taking into account the impact of radiative loss shown by the black circles and red squares, respectively. (c) Inferred yield amplification vs $\chi_{\mathrm{no}\,\alpha}$ with regions of burning hot spot and plasma denoted as defined by [30]. Green and red circles indicate experiments N170821 and N170601 conducted with a 10 and 5 μm fill tube, respectively. The red and blue diamonds denote experiments shown in Fig. 3(a). Higher yield amplifications can be obtained in simulations of implosions of similar adiabat (2.9 vs 3), without drive asymmetries and with 1.15 times larger capsules that absorb ~1.15 times more energy and obtain a velocity 1.09 times larger than experiments reported here.

to observations. Both data and simulations suggest that further decreasing the fill tube perturbation, given the current level of other degradations, will only lead to modest improvements in performance. However, as will be discussed, reducing the fill tube perturbation as much as possible is still important, as it will be essential to achieve higher performance as other degradation mechanisms are alleviated.

To quantify the impact of radiative loss on fusion yield, an analytic scaling for the expected yield [31] was adapted to include the mix degradation, and can be written as

$$Y \propto p_{\mathrm{abl}}^{16/25} v_{\mathrm{imp}}^{67/15} S^{14/3} a^{-36/25} \delta^{14/15}. \tag{2}$$

Here, p_{abl}. is the ablation pressure 500 ps before stagnation, v_{imp}. is the peak implosion velocity, S is the initial capsule scale, and a is the DT fuel in-flight adiabat. The degradation term, δ, can be written as $\delta = \exp[-\int_0^t Q_{\mathrm{mix}}/(c_{\mathrm{DT}}T)\mathrm{d}t]$ and follows from Eq. (12) in [31] with $Q_{\mathrm{other}} = Q_{\mathrm{mix}}$. Using an adiabatic assumption, as the mix radiative losses are small compared to the internal energy, and in the limit that $Q_{\mathrm{mix}} \ll Q_{\mathrm{DT}}$, this term reduces to $\delta \approx (1 - m.f.\eta T\tau)$. Here the emission mix fraction is defined as $m.f. = Q_{\mathrm{mix}}/Q_{\mathrm{rad}} \approx Q_{\mathrm{mix}}/Q_{\mathrm{DT}}$, with $Q_{\mathrm{DT}} \propto \rho_{\mathrm{DT}} T^{1/2}$ and η is a constant related to the total rate of emission with units $(T\tau)^{-1}$, where T and τ are the ion temperature and emission duration, respectively [32]. When the radiative loss from the mix is a small fraction of the total radiative loss, as it is here [22], the yield degradation is expected to scale nearly linearly with the mix fraction.

Figure 3(b) shows a comparison between the observed and the expected yield utilizing Eq. (2) with and without the degradation associated with radiative loss from mix for 14 experiments conducted with HDC ablators. The radiation drive measured by the DANTE diagnostic [33], together with a rocket model[34], is used to estimate p_{abl}. and v_{imp}. for each implosion. The adiabat term was neglected as it is a relatively low power, and all the experiments were designed to have nearly the same value. The red squares denote the yield expectation neglecting the mix degradation. Here, the expected yield is normalized to the experiment with the least amount of observed mix. The black circles in Fig. 3(b) show the relationship between the observed and expected yield taking into account the impact of radiative loss from mix using the observed mix fraction for each experiment together with the measured rate of relative yield decrease with mix fraction from Fig. 3(a). As Fig. 3(b) shows, this results in a more accurate yield expectation, decreasing the χ^2 between the observation and expectation from 1.6 to 0.4. While there are other effects varying shot-to-shot in these implosions, the fact that radiative loss can account for most of the observed variability in yield indicates that it is a dominant term in the implosion performance.

Figure 3(c) shows that the radiative loss from the fill tube perturbation significantly impacts the proximity to ignition, as defined using the relationship between the yield amplification, y_{amp}, and the $\chi_{\mathrm{no}\,\alpha}$ ignition metric [30]. Here y_{amp}. is defined to be the observed yield divided by the simulated yield with α particle deposition turned off. Simulations with α particle deposition turned on, with the inferred drive asymmetries, reduced compression, and fill tube perturbations reproduced the observed yield to within ~25%. For a given y_{amp}, $\chi_{\mathrm{no}\,\alpha}$ can be calculated using the relationships detailed in [30]. Decreasing the fill tube diameter from 10 to 5 μm increased $\chi_{\mathrm{no}\,\alpha}$ from 0.49 to 0.72, which is 92% of

the $\chi_{\mathrm{no}\,\alpha}$ required to enter into the burning hot spot regime. Additional sources of localized radiative loss on two of the four repeated experiments conducted with a 5 μm fill tube degraded the yield [Fig. 3(a)], and therefore y_{amp}. and $\chi_{\mathrm{no}\,\alpha}$ obtained in Fig. 3(c). A reduction of the fill tube diameter from 5 to 2 μm decreased the perturbation size [22] but did not lead to an increase in y_{amp}. This indicates that the fill tube perturbation no longer dominates the degradation and that other degradation mechanisms must be alleviated before further yield increases can be obtained. Using the model of the fill tube perturbation validated by this work [35], simulations of implosions at similar adiabats, but with 1.15 times larger capsules that reach 1.09 times higher velocities, were performed. These simulations [22] suggest that in addition to increasing the velocity and improving the symmetry of the implosion, decreasing the fill tube diameter to 2 μm is essential to reach yield amplifications >3.5 times with the current NIF and HDC implosion designs.

In summary, the radiative loss and impact to plasma conditions from a spatially localized mix injected into the reacting plasma has been quantified using neutron and x-ray emission to reconstruct hot spot conditions. The ability to reconstruct the hot spot density and temperature profile will also enable the study of a broader class of physical processes that determines the compressibility, conduction rates, and alpha stopping power within the hot spot. The updated analytic yield scaling indicates that radiative loss from a localized mix has been the dominant source of observed yield variations. This work significantly advances our ability to isolate and assess the impact of other degradations in ICF implosions.

We thank D. Callahan, M. J. Edwards, W. W. Hsing, O. L. Landen, A. J. Mackinnon, N. B. Meezan, and R. P. J. Town for enabling and supporting this work. Additionally we thank B. Bachmann, L. R. Benedetti, N. Izumi, S. R. Nagel, and J. E. Ralph for insightful technical discussions and A. Nikroo, J. Biener, T. Bunn, J. Crippen, C. Kong, N. Rice, and M. Stadermann from LLNL and from General Atomics for their efforts in fabricating the targets used in this work. This work was performed under the auspices of the U.S. Department of Energy (DOE) under Contract No. DE-AC52-07NA27344.

[1] National Research Council, *Burning Plasma: Bringing a Star to Earth* (The National Academies Press, Washington, DC, 2004).
[2] R. Betti and O. A. Hurricane, Nat. Phys. **12**, 435 (2016).
[3] ITER Organization, *ITER Research Plan within the Staged Approach* (2018), https://www.iter.org/technical-reports.
[4] J. Lindl, Phys. Plasmas **2**, 3933 (1995).
[5] M. J. Edwards *et al.*, Phys. Plasmas **20**, 070501 (2013).
[6] S. Le Pape *et al.*, Phys. Rev. Lett. **120**, 245003 (2018).
[7] O. A. Hurricane *et al.*, Nature (London) **506**, 343 (2014).
[8] L. Divol *et al.*, Phys. Plasmas **24**, 056309 (2017).
[9] T. Ma *et al.*, Phys. Rev. Lett. **111**, 085004 (2013).
[10] S. P. Regan *et al.*, Phys. Rev. Lett. **111**, 045001 (2013).
[11] J. Biener *et al.*, Nucl. Fusion **49**, 112001 (2009).
[12] L. B. Hopkins *et al.*, Plasma Phys. Controlled Fusion **61**, 014023 (2019).
[13] T. Ma *et al.*, Phys. Plasmas **24**, 056311 (2017).
[14] J. Edwards, M. Marinak, T. Dittrich, S. Haan, J. Sanchez, J. Klingmann, and J. Moody, Phys. Plasmas **12**, 056318 (2005).
[15] D. S. Clark, A. L. Kritcher, S. A. Yi, A. B. Zylstra, S. W. Haan, and C. R. Weber, Phys. Plasmas **25**, 032703 (2018).
[16] L. A. Pickworth *et al.*, Phys. Plasmas **25**, 054502 (2018).
[17] P. Chang, R. Betti, B. K. Spears, K. S. Anderson, J. Edwards, M. Fatenejad, J. D. Lindl, R. L. McCrory, R. Nora, and D. Shvarts, Phys. Rev. Lett. **104**, 135002 (2010).
[18] E. I. Moses *et al.*, Fusion Sci. Technol. **69**, 1 (2016).
[19] F. E. Merrill *et al.*, Rev. Sci. Instrum. **83**, 10D317 (2012).
[20] S. M. Glenn *et al.*, Rev. Sci. Instrum. **83**, 10E519 (2012).
[21] M. A. Barrios *et al.*, Phys. Plasmas **20**, 072706 (2013).
[22] See Supplemental Material at http://link.aps.org/supplemental/10.1103/PhysRevLett.124.145001 for additional details on experimental measurements and simulations.
[23] P. Volegov *et al.*, Rev. Sci. Instrum. **85**, 023508 (2014).
[24] L. Divol *et al.*, Phys. Plasmas (to be published).
[25] H. Scott and S. Hansen, High Energy Density Phys. **6**, 39 (2010).
[26] B. Bachmann *et al.*, Phys. Rev. E (to be published).
[27] E. Marley *et al.*, Phys. Plasmas (to be published).
[28] S. Atenzi and J. Meyer-ter Vehn, *The Physics of Inertial Fusion* (Oxford University Press, 2004).
[29] M. M. Marinak, G. D. Kerbel, N. A. Gentile, O. Jones, D. Munro, S. Pollaine, T. R. Dittrich, and S. W. Haan, Phys. Plasmas **8**, 2275 (2001).
[30] R. Betti, A. R. Christopherson, B. K. Spears, R. Nora, A. Bose, J. Howard, K. M. Woo, M. J. Edwards, and J. Sanz, Phys. Rev. Lett. **114**, 255003 (2015).
[31] O. A. Hurricane *et al.*, Plasma Phys. Controlled Fusion **61**, 014033 (2019).
[32] O. A. Hurricane (private communication).
[33] E. L. Dewald *et al.*, Rev. Sci. Instrum. **75**, 3759 (2004).
[34] Y. Saillard, Nucl. Fusion **46**, 1017 (2006).
[35] C. Weber *et al.*, Phys. Plasmas **27**, 032703 (2020).